C-H Bond Chlorination Using Nickel(II) Complexes of Tetradentate Amido-Quinoline Ligands

Sanjay Adhikari,[a] Aniruddha Sarkar[b] and Basab Bijayi Dhar[a]*

[a]Department of Chemistry Shiv Nadar University Uttar Pradesh 201314 India

[b]Department of Chemistry indian-Institute of Science, Education and Research Kolkata Mohanpur 741246, India

Email: basab.dhar@snu.edu.in, basabbijayi@gmail.com

Supplementary Information

Table of Contents

Physical methods and materials

All commercially available reagents (Sigma Aldrich Co., Finar, Chempure(P) Ltd., Rankem etc.) were used without further purification. All the solvents were of HPLC grade and was dried and distilled prior to use according to standard procedures. ^{1}H and ^{13}C NMR spectra were recorded on a 400 MHz or 100 MHz Bruker NMR spectrometer respectively. Chemical shifts are given as the δ value (ppm) with reference to tetramethylsilane (TMS) as an internal standard. High resolution mass spectroscopy (HRMS) were carried out using 6540 UHD Accurate-Mass Q-TOF LC/MS system (Agilent Technologies, Santa Clara, CA, USA) equipped with Agilent 1290 UPLC system. Mixture of organic compounds were identified by Agilent 5977B GC/MSD equipped with a HP-5 MS capillary column (30 m x 0.32 mm x 0.25 μm) and quantified using Agilent 7890B GC system equipped with a HP-5 capillary column (30 m x 0.32 mm x 0.25 μm) by using a calibration curve obtained with authentic compounds. The products were quantified by using GC(FID) analysis.

Structure determination by X-ray crystallography

Crystal structures of ligands and nickel compounds were determined by measuring X-ray diffraction data on D8 Venture Bruker AXS single crystal X-ray diffractometer equipped with CMOS PHOTON 100 detector having monochromatised microfocus sources (Mo−Kα = 0.71073 Å). All the crystal data were collected at room temperature. Structures were solved using SHELX program implemented in APEX3.[1-4] The non-H atoms were located in successive difference Fourier syntheses and refined with anisotropic thermal parameters. All the hydrogen atoms were placed at the calculated positions and refined using a riding model with appropriate HFIX commands.Further to confirm the coordination of the amido-quinoline ligands to the nickel centre single crystal X-ray analysis was carried out to explore its geometry. The detail regarding data collection and structure refinement parameters are summarized in (Table S1) and geometrical parameters including bond lengths and bond angles are listed in (Table S2). Single crystals of amido-quinoline ligands (L1 and L2) suitable for X-ray diffraction were obtained by slow evaporation from DCM/Hexane solution, whereas for complexes (**1** and **2**) single crystals were obtained from DMF solution.

Electrochemical measurements

Cyclic voltammetry (CV) experiments were conducted in CHI-660 potentiostat, using a glassy carbon working electrode, a platinum wire counter electrode, and an $Ag/AgNO_3$ (0.01

M) reference electrode in DCM medium ([Ni(II)$L_{1/2}$] = 1 mM, scan rate: 0.1 Vs^{-1}. The supporting electrolyte was 0.1 M $^{n}Bu_4NPF_6$ (^{n}Bu = n-butyl). The potential was referenced to the $Ag/AgNO_3$ couple by the addition of an Fc standard to the solution. The respective plots are shown in Fig. S12.

Catalytic oxidation of alkanes with NaOCl

A mixture of nickel complexes (0.25 μmol), substrates (0.25 mmol) and NaOCl (0.25 mmol, 500 μL) were added in 1 mL of CH_3CN:CH_2Cl_2 mixture (8:2 v/v) and stirred vigorously at RT for 30 min under N_2. Then the nickel complex was removed by passing the solution through a short plug of neutral alumina. A fraction of the resulting mixture was analysed by GC(FID) and the products were identified by GC-MS. The products were quantified from calibration curve of authentic compounds. The TON value are reported in Table 2 and 3.

Chromatographic methods.

Chromatographic separation of the various products shown in this work was performed using the following chromatographic methods:

Column: - Agilent 7890B GC system equipped with a HP-5 capillary column (30 m x 0.32 mm x 0.25 μm); Agilent 5977B GC/MSD equipped with a HP-5 MS capillary column (30 m x 0.32 mm x 0.25 μm)

For cyclohexane, toluene, ethyl benzene

Detector: Flame ionization detector (FID)
- Zero air (carrier gas) 300 mL/min
- H_2 (fuel gas) 30 mL/min
- N_2 (make up) 25 mL/min

Initial column temperature: 60 °C
Final column temperature: 200 °C
Temperature ramp: 10 °C/min
Injector temperature: 225 °C
- Septum purge flow: 3 mL/min
- Total flow: 34 mL/min
- Split ratio: 30:1

Detector temperature 250 °C

For 4-methyl biphenyl

Detector: Flame ionization detector (FID)
- Zero air (carrier gas) 300 mL/min
- H_2 (fuel gas) 30 mL/min
- N_2 (make up) 25 mL/min

Initial column temperature: 60 °C
Final column temperature: 280 °C
Temperature ramp: 10 °C/min
Injector temperature: 250 °C

Septum purge flow: 3 mL/min
Total flow: 34 mL/min
Split ratio: 50:1
Detector temperature 280 ℃

For Adamantane

Detector: Flame ionization detector (FID)
Zero air (carrier gas) 300 mL/min
H_2 (fuel gas) 30 mL/min
N_2 (make up) 25 mL/min
Initial column temperature: 60 ℃
Final column temperature: 250 ℃
Temperature ramp 1: 10 ℃/min to 120 ℃/min
Temperature ramp 2: 10 ℃/min to 250 ℃/min
Injector temperature: 225 ℃
Septum purge flow: 3 mL/min
Total flow: 34 mL/min
Split ratio: 30:1
Detector temperature 250 ℃

For 2,3-dimethyl butane

Detector: Flame ionization detector (FID)
Zero air (carrier gas) 300 mL/min
H_2 (fuel gas) 30 mL/min
N_2 (make up) 25 mL/min
Initial column temperature: 40 ℃
Final column temperature: 200 ℃
Temperature ramp: 10 ℃/min to 200 ℃/min
Injector temperature: 225 ℃
Septum purge flow: 3 mL/min
Total flow: 34 mL/min
Split ratio: 30:1
Detector temperature 250 ℃

Synthesis of ligands

8-amino quinoline (720.85 mg, 5 mmol) and trimethylamine (1.01 mL, 5 mmol) were dissolved in dry THF 20 mL under N_2 atmosphere at 0 ℃. Then the respective acyl chloride (2.5 mmol) 2,2′-dimethyl malonylchloride in case of (L1) and N-formyl methylamine (L2) predissoved in 20 mL of dry THF was added dropwise at 0 ℃ over a period of 15 minutes under vigorous stirring. Over the course of time a formation of white precipitate of triethylammonium chloride started, indicates the progress of amide coupling. After completing the drop wise addition, the reaction mixture was brought to room temperature (RT) and stirred overnight. The reaction mixture was filtered over celite to remove the salt and the filtrate was

evaporated to dryness and the residue was re-dissolved in 100 mL of DCM and washed with aqueous $NaHCO_3$ (3 × 50 mL) and the solvent was evaporated to dryness. The ligands were further purified by column chromatography using 40 % EtOAc in hexane to afford ligands as pure white crystals.

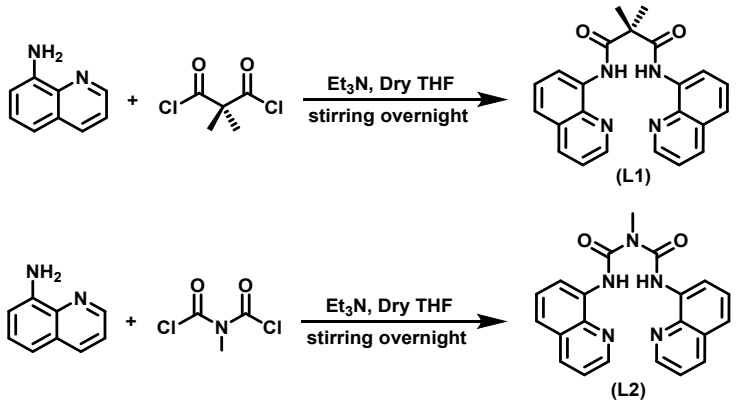

Scheme 1 Synthesis of amido-quinoline ligands.

Dimethyl *N; N*'-Bis(8-quinolyl)malonamide (L1)

Color: White crystals; Yield 1.15 g (60%) ^{1}H-NMR (400 MHz, $CDCl_3$): δ = 10.95 (s, 2H, NH), 8.84-8.88 (m, 4H), 8.14 (dd, 2H, *J* = 4 and 8 Hz), 7.51-7.57 (m, 4H), 7.45-7.48 (m, 2H), 1.94 (s, 6H, CH_3); ^{13}C NMR (100 MHz, $CDCl_3$): δ = 171.61, 148.56, 138.97, 136.15, 134.44. 127.91, 127.22, 121.86, 121.61, 116.72, 52.72, 24.09; HR-MS (m/z) [Found (calcd)]: [385.1649 (385.1660)] $[M + H]^+$.

Methyl *N; N*'-Bis(8-quinolyl)formylamide (L2)

Color: White crystals; Yield 1.05 g (57%) ^{1}H-NMR (400 MHz, $CDCl_3$): δ = 11.63 (s, 2H, NH), 8.94 (dd, 2H, *J* = 4 and 4 Hz), 8.79 (d, 2H, *J* = 4 Hz), 8.20 (dd, 2H, *J* = 4 and 4 Hz), 7.60 (d, 2H, *J* = 8 Hz), 7.55 (d, 2H, *J* = 8 Hz), 7.47-7.51 (m, 2H), 3.78 (s, 3H, CH_3); ^{13}C NMR (100 MHz, $CDCl_3$): δ = 153.75, 148.59, 139.16, 136.30, 135.03, 128.08, 127.33, 121.55, 121.37, 116.61, 30.75; HR-MS (m/z) [Found (calcd)]: [371.1483 (372.1455)] $[M + H]^+$.

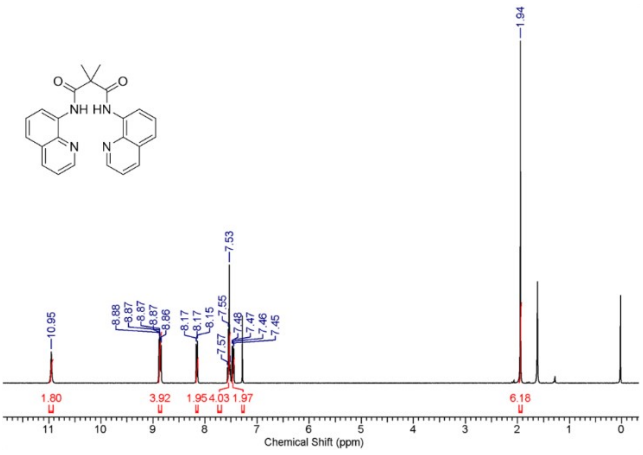

Fig. S1 ^{1}H-NMR spectrum of L1.

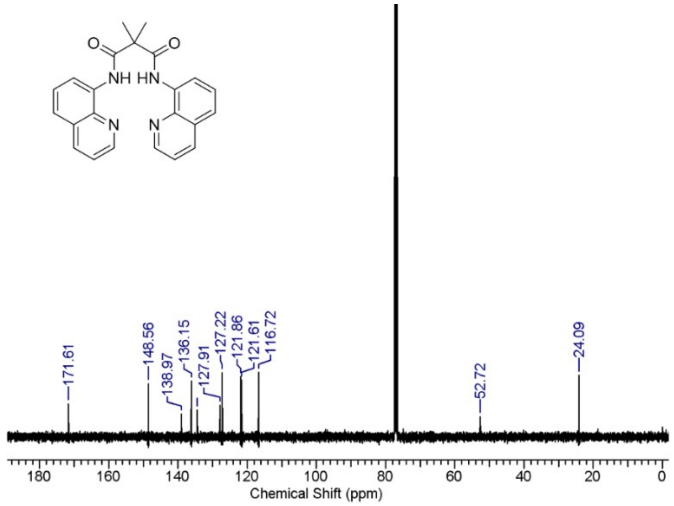

Fig. S2 ^{13}C-NMR spectrum of L1.

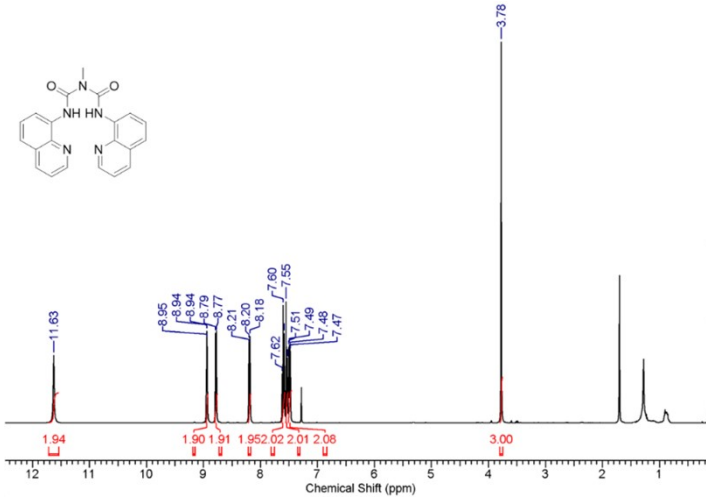

Fig. S3 ^{1}H-NMR spectrum of L2.

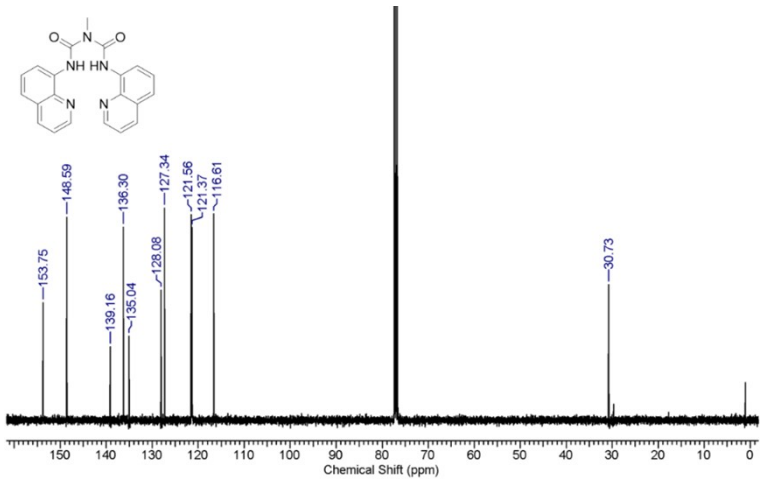

Fig. S4 ^{13}C-NMR spectrum of L2.

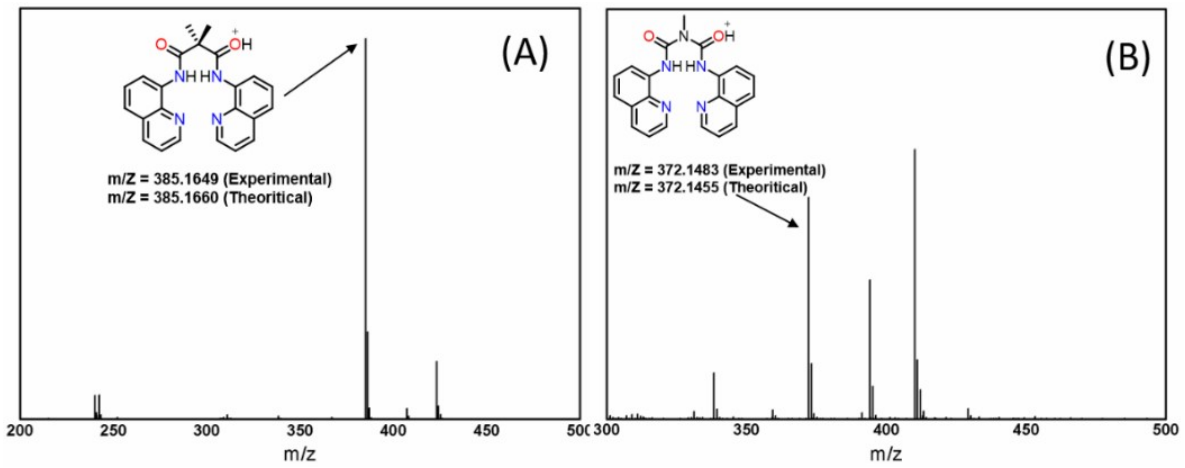

Fig. S5 (A) HR-MS of (L1) and (B) HR-MS of L2.

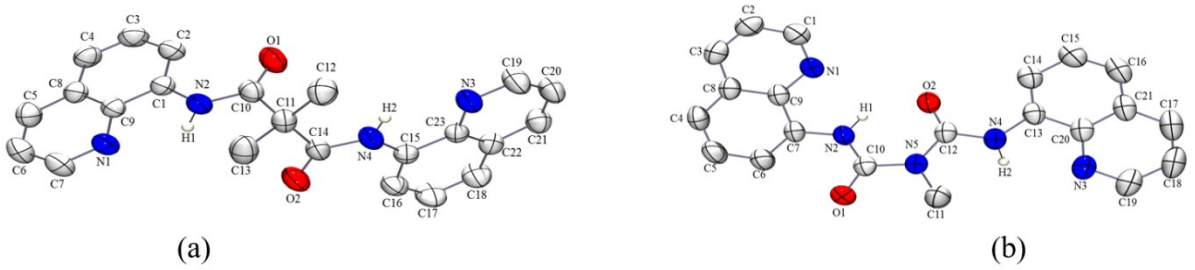

Fig. S6. (a) ORTEP plot of (L1) and (b) ORTEP plot of (L2) with 50% probability thermal ellipsoids. Hydrogen atoms (except on N2 and N4) are omitted for clarity.

Synthesis and Characterization of Ni(II)-amidoquinoline complexes

Two equivalents of trimethylamine or sodium hydride was added in to a solution of ligands (**L1** and **L2**) (0.3 mmol) in 5 mL of dry DMF under N_2 atmosphere and stirred. It resulted a yellow colored solution. After 15 minutes $NiCl_2.6H_2O$ (0.32 mmol) was added as a solid and a dark orange coloration was observed (Fig. S7). The mixture was stirred at room temperature for 4 hours. Then this solution was filtered over celite and the solution was directly kept for crystallization. Crystals of pure complexes were obtained within one week (Table S1, Fig. 1). ^1H and ^{13}C NMR of **1** and **2** were given in Fig. S8-S10. Cyclic voltamogram and HR-MS of **1** and **2** were described in Fig. S11and Fig. S12 respectively.

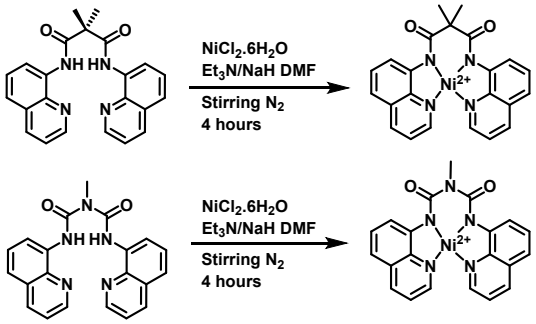

Scheme 2 Synthesis of Ni(II) complexes.

Complex (1) $[Ni(L1)]^{2+}$

Dark red crystals; Yield 68 mg (51%) ^{1}H-NMR (400 MHz, $CDCl_3$): δ = 9.05 (d, 2H, *J* = 8 Hz), 8.36 (d, 2H, *J* = 8 Hz), 7.95 (d, 2H, *J* = 4 Hz), 7.59 (t, 2H, *J* = 8 Hz), 7.47 (t, 2H, *J* = 8 Hz), 1.83 (s, 6H, CH_3); ^{13}C NMR (100 MHz, $CDCl_3$): δ = 180.58, 148.87, 148.57, 144.94, 139.21, 130.47, 128.62, 121.87, 120.98, 117.84, 54.0, 27.99; HR-MS (m/z) [Found (calcd)]: [441.0838 (441.0856)]; UV/vis {CH_3CN:DCM (8:2), λ_{max}, nm (ε/10^{-4} M^{-1} cm^{-1})}: 258 (19600 M^{-1} cm^{-1}), 279 (15800 M^{-1} cm^{-1}), 318 (3500 M^{-1} cm^{-1}), 426 (7100 M^{-1} cm^{-1}).

Complex (2) $[Ni(L2)]^{2+}$

Dark orange crystals; Yield 64 mg (50%) ^{1}H-NMR (400 MHz, $CDCl_3$): δ = 9.07 (d, 2H, *J* = 8 Hz), 8.37 (d, 2H, *J* = 8 Hz), 8.02 (d, 2H, *J* = 4 Hz), 7.61 (t, 2H, *J* = 8 Hz), 7.48 (t, 2H, *J* = 8 Hz), 7.32 (d, 2H, *J* = 8 Hz), 3.43 (s, 3H, CH_3); HR-MS (m/z) [Found (calcd)]: [428.0648 (428.0652)]; UV/vis {CH_3CN, λ_{max}, nm (ε/10^{-4} M^{-1} cm^{-1})}: 240 (24500 M^{-1} cm^{-1}), 264 (19800 M^{-1} cm^{-1}), 320 (2300 M^{-1} cm^{-1}), 421 (4600 M^{-1} cm^{-1}).

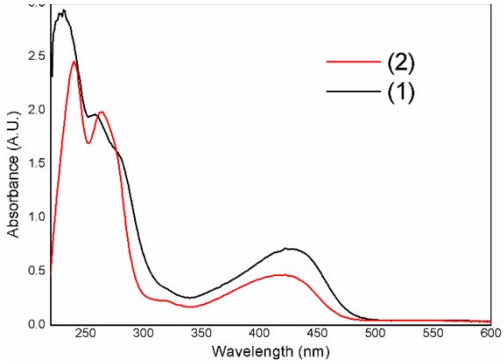

Fig. S7 UV-Vis spectra of complexes (**1** and **2**) in CH_3CN:CH_2Cl_2 (8:2) (0.1 mM).

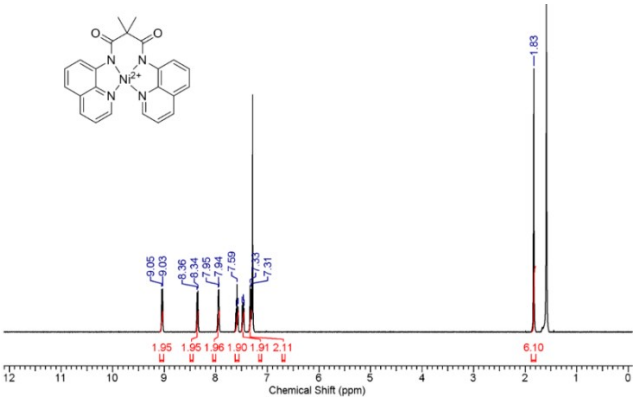

Fig. S8 ^{1}H-NMR spectrum of **1**.

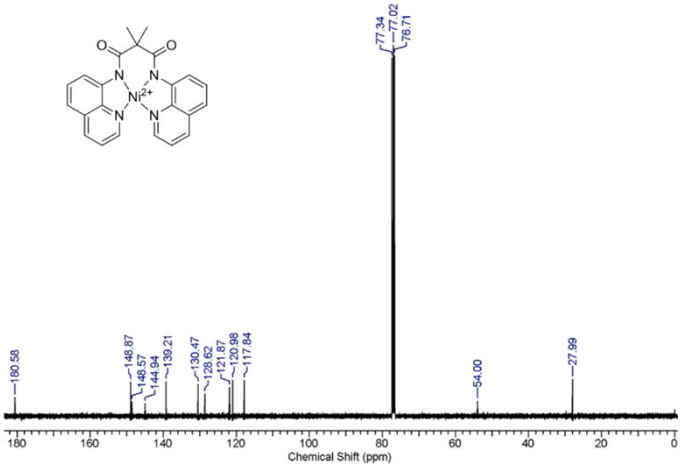

Fig. S9 ^{13}C-NMR spectrum of complex **1**.

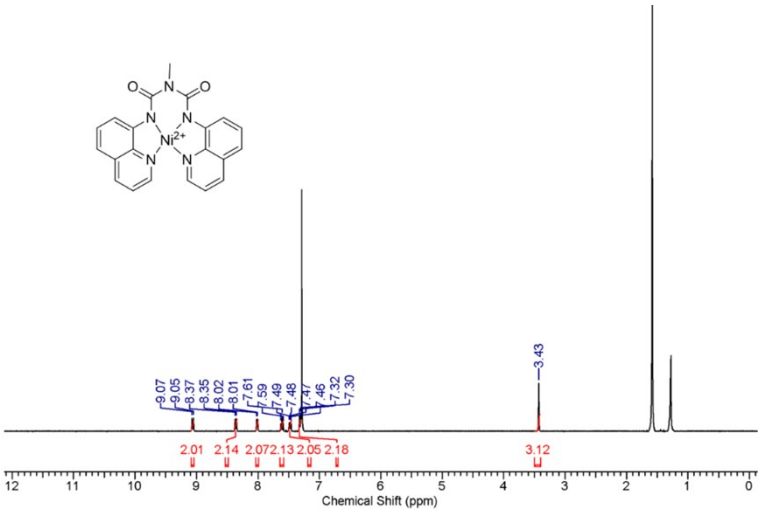

Fig. S10 ^{1}H-NMR spectrum of complex **2**.

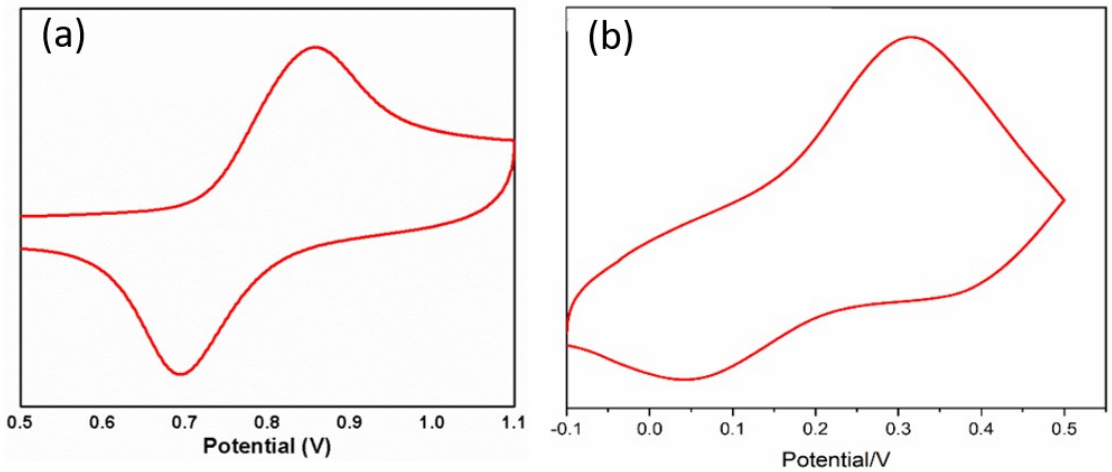

Fig. S11 (a) Cyclic voltamogram of (**1**) and (b) (**2**) (1 mM) in DCM at 25 °C Supporting electrolyte: NBu_4PF_6 (0.05 M); Reference electrode: Ag/Ag^+; working electrode: Pt-sphere; Counter electrode: Pt wire; Scan rate: 100 mV s^{-1}.

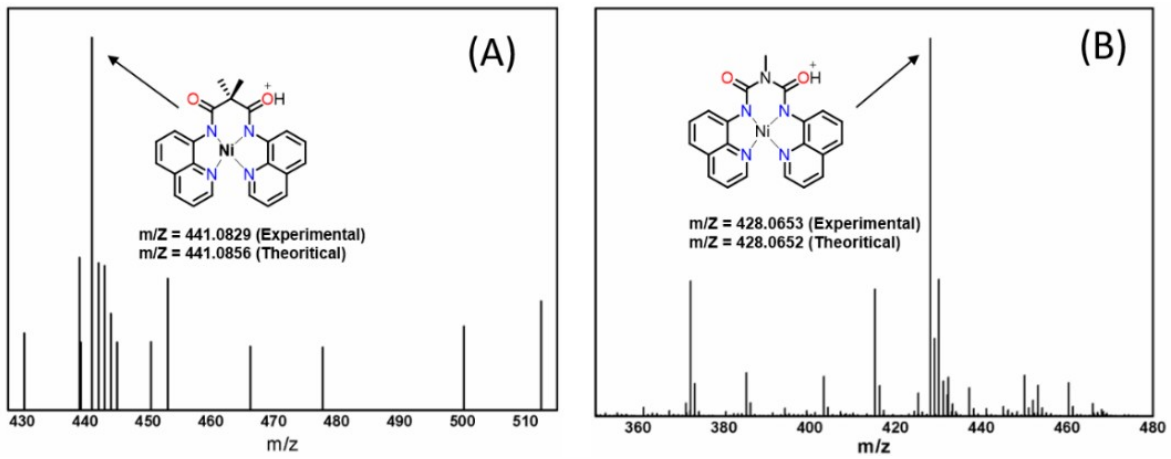

Fig. S12. (A) HR-MS of **1** and (B) HR-MS of **2**.

Table S1 Crystal data and structure refinement parameters of complexes.

Compounds	L1	L2	**1**	**2**
Empirical formula	$C_{22}H_{18}N_4O_2$	$C_{22}H_{15}N_4O_2$	$C_{23}H_{18}N_4O_2Ni$	$C_{21}H_{15}N_5O_2Ni$
Formula weight	384.43	371.40	441.12	428.07
Temperature (K)	297(2)	297 (2)	297(2)	299(2)
Wavelength (Å)	0.71073	0.71073	0.71073	0.71073
Crystal system	triclinic	monoclinic	monoclinic	triclinic
Space group	*P-1*	*P2₁/n*	*P2₁/c*	*P-1*
a (Å)/α (°)	7.835(6)/100.17(2)	8.2961(3)/90	10.4454(3)/90	8.0529(19)/96.460(14)
b (Å)/β (°)	7.929(5)/92.23(3)	19.4180(8)/109.1040(10)	14.2526(4)/98.21(10)	10.359(3)/109.436(10)
c (Å)/γ (°)	15.763(11)/98.55(3)	11.7921(5)/90	98.2100(10)/90	11.497(3)/103.717(10)
Volume (Å^3)	951.0(12)	1795.01(12)	1950.36(10)	859.2(4)
Z	2	34	4	2
Density (calc) (Mg/m^{-3})	1.342	1.374	1.502	1.655
Absorption coefficient (μ) (mm^{-1})	0.088	0.093	1.023	1.160
F(000)	404.0	776.0	912	440.4
Crystal size (mm^3)	0.21 x 0.11 x 0.06	0.23 x 0.12 x 0.05	0.23 x 0.10 x 0.05	0.21 x 0.12 x 0.05
Theta ranges for data collection	2.631-25.174°	2.098-23.553°	2.434 - 26.39°°	1.921-31.410°
Index ranges	-9<=h<=9, -9<=k<=9, -18<=l<=18	-9<=h<=9, -21<=k<=21, -13<=l<=13	-13<=h<=13, -17<=k<=17, -16<=l<=16	-11<=h<=11, -15<=k<=15, -16<=l<=16
Reflections collected	29657	20692	25752	33649
Independent reflections	3422 [R(int) = 0.0420]	2680 [R(int) = 0.0359]	3977 [R(int) = 0.0371]	5637 [R(int) = 0.0413]
Data/restraints/parameters	3422/0/265	2680/0/255	3977/0/273	5637/0/263
Goodness-of-fit on F^2	0.983	2.652	1.017	0.668
Final R indices [I>2sigma(I)]	R1 = 0.0380 wR$_2$ = 0.0837	R1 = 0.0347 wR$_2$ = 0.0888	R1 = 0.0319wR$_2$ = 0.0725	R1 = 0.0322 wR$_2$ = 0.0760
R indices (all data)	R1 = 0.0559 wR$_2$ = 0.0962	R1 = 0.0448 wR$_2$ = 0.0977	R1 = 0.0494 wR$_2$ = 0.0839	R1 = 0.0463 wR$_2$ = 0.0832
Largest diff peak and hole (e Å^{-3})	0.134 and -0.132	0.110 and -0.119	0.260 and -0.232	0.294 and -0.351
CCDC No.	2107880	2108322	2108323	2108324

Table S2 Selected bond lengths (Å) and bond angles (°) of complexes

	Bond length [Å]	
	1	**2**
Ni-N(1)	1.9209(16)	1.913(14)
Ni-N(2)	1.8806(16)	1.859(14)
Ni-N(3)	1.909(16)	1.920(14)
Ni-N(4)	1.8801(15)	1.862(13)
Ni-N(5)	----	3.170(13)
	Bond angles [°]	
N(1)-Ni-N(2)	85.09(1)	84.43(7)
N(1)-Ni-N(4)	174.8(1)	173.82(7)
N(3)-Ni-N(4)	85.2(1)	85.40(7)
N(3)-Ni-N(2)	162.9(1)	164.04(7)
N(2)-Ni-N(4)	93.7(1)	92.08(7)
N(1)-Ni-N(3)	98.5(1)	99.34(7)
Tetrahedral distortion parameter (τ_4)	0.159	0.157

Table S3 Optimization of C-H chlorination[a] using **1**

Entry	Catalyst	Oxidant (eq)	TON
1	**1**	0.5	108
2	**1**	1	165
3	**1**	1.5	137
4	**1**	2eq	103
5[b]	**1**	1eq	146
6[c]	**1**	1eq	182
7[d]	-	1eq	33
8[e]	$NiCl_2.6H_2O$	1eq	36
9[f]	$NiCl_2.6H_2O$ + L1	1eq	104

[a]General reaction conditions 0.25 µmol Ni(L1), cyclohexane 0.25 mmol in CH_3CN:CH_2Cl_2 (8:2 v/v) 1mL under N_2 stirring at RT for 30 mins. [b]At pH 7.4; [c]At pH 9.2; [d]NaOCl only; [e]NaOCl + $NiCl_2.6H_2O$, [f]$NiCl_2.6H_2O$ (0.25 µmol) + L1(0.25 µmol); TON = mmol of product/mmol of catalyst. TON determined using GC (FID) and products identified using GC-MS.

Gas Chromatography (GC) Analysis

Fig. S13 GC trace for oxidation of cyclohexane using **1** and 0.5 eq. NaOCl (X axis: in minute; Y axis: % abundance), entry 1 of Table 2.

Fig. S14 GC trace for oxidation of cyclohexane using **1** and 1 eq. NaOCl (X axis: in minute; Y axis: % abundance), entry 2 of Table 2.

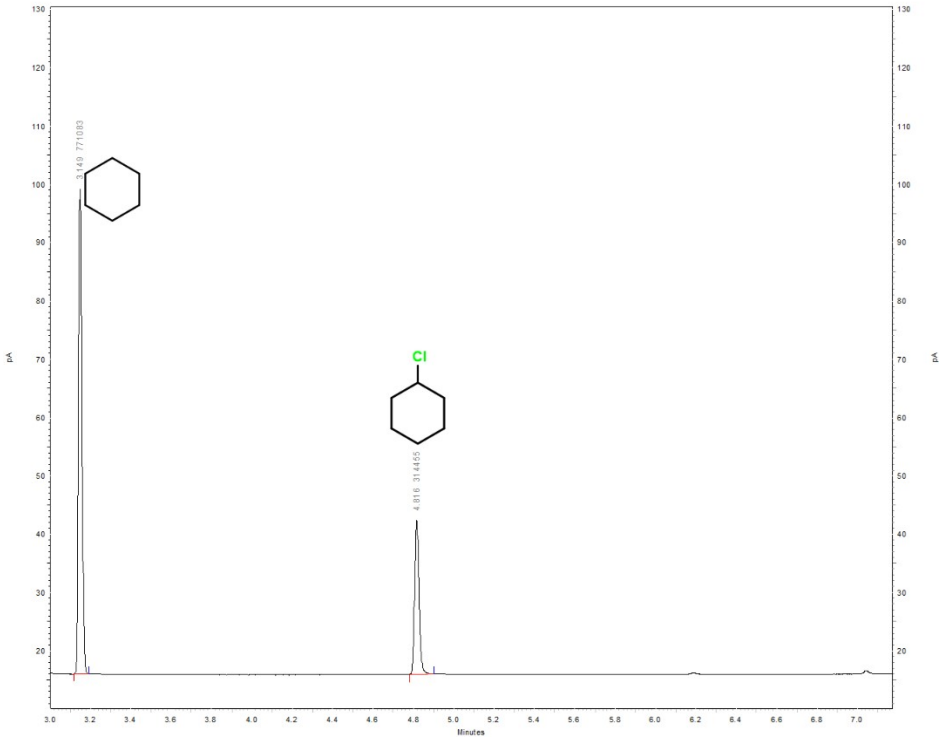

Fig. S15 GC trace for oxidation of cyclohexane using **1** at pH 7.4 (X axis: in minute; Y axis: % abundance); entry 5 of Table 2.

Fig. S16 GC trace for oxidation of cyclohexane using **1** at pH 9.2 (X axis: in minute; Y axis: % abundance), entry 6 of Table 2.

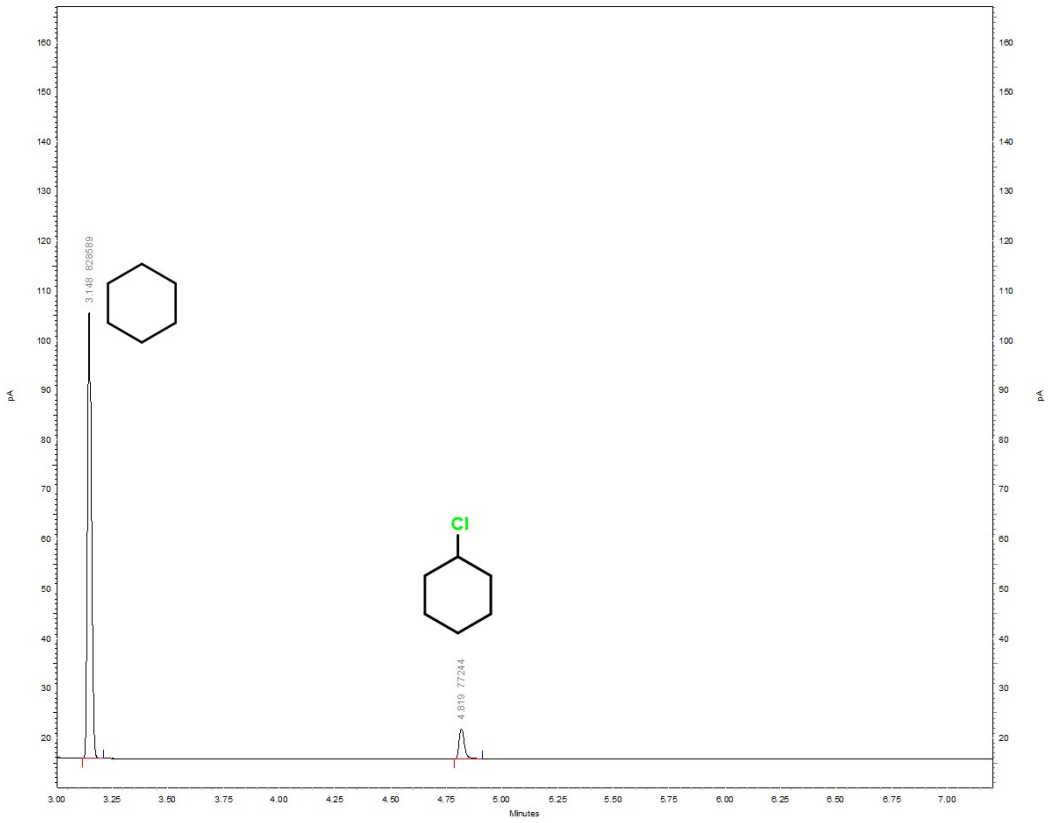

Fig. S17 GC trace for oxidation of cyclohexane using only NaOCl (X axis: in minute; Y axis: % abundance), entry 7 of Table 2.

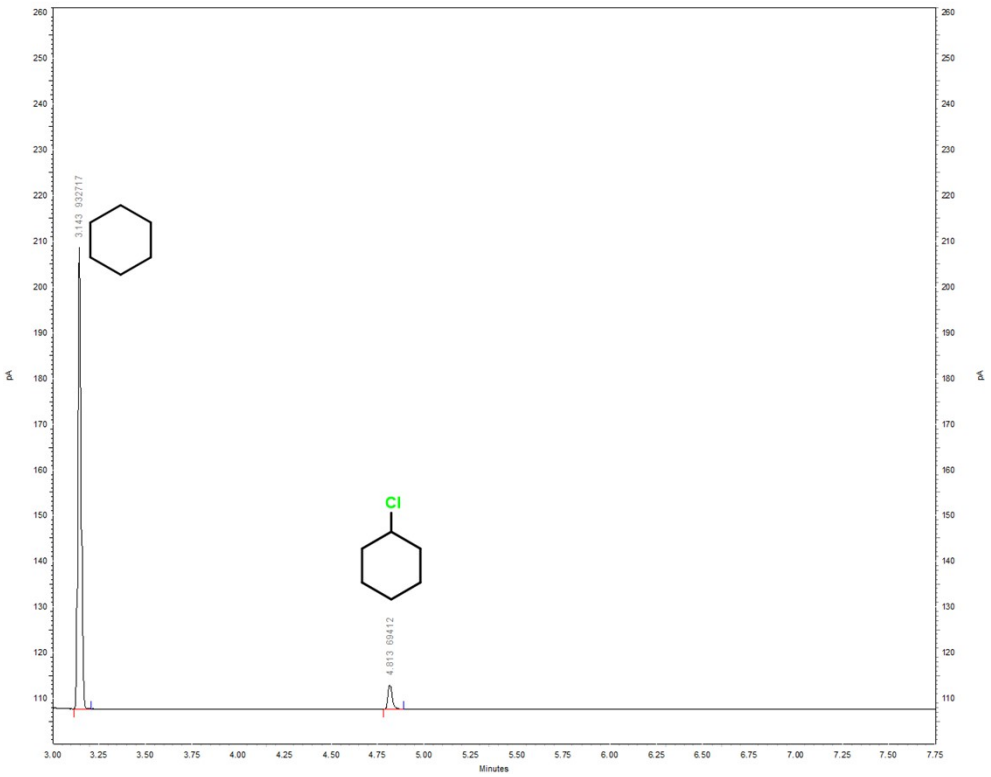

Fig. S18 GC trace for oxidation of cyclohexane using $NiCl_2.6H_2O$ (X axis: in minute; Y axis: % abundance), entry 8 of Table 2.

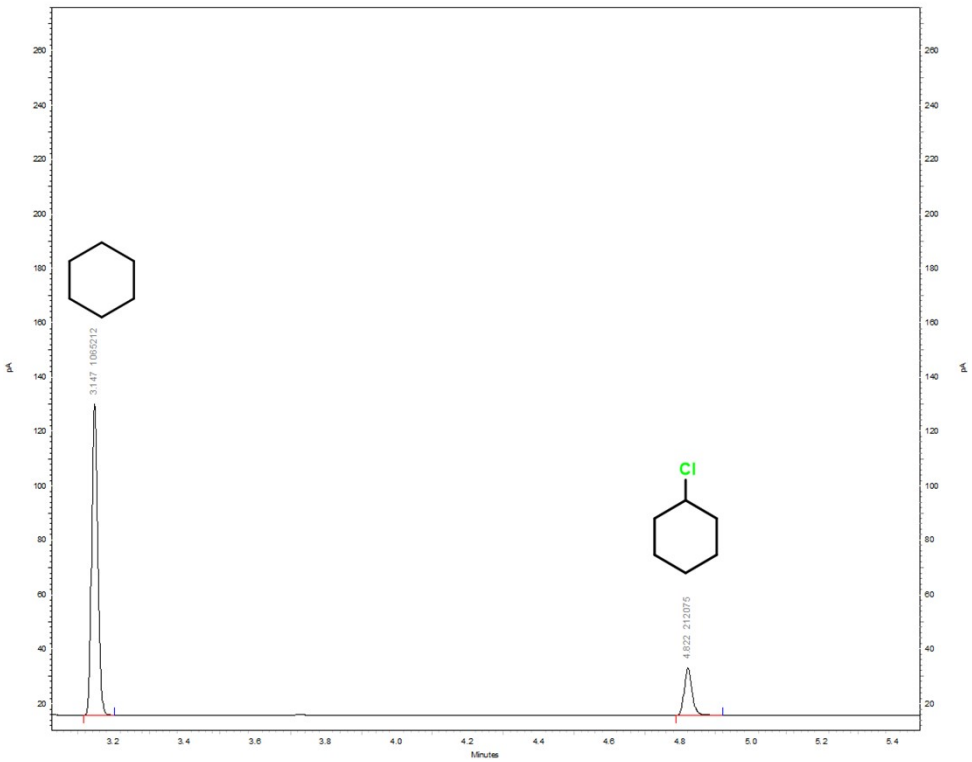

Fig. S19 GC trace for oxidation of cyclohexane using $NiCl_2.6H_2O$ + L1 (X axis: in minute; Y axis: % abundance), entry 9 of Table 2.

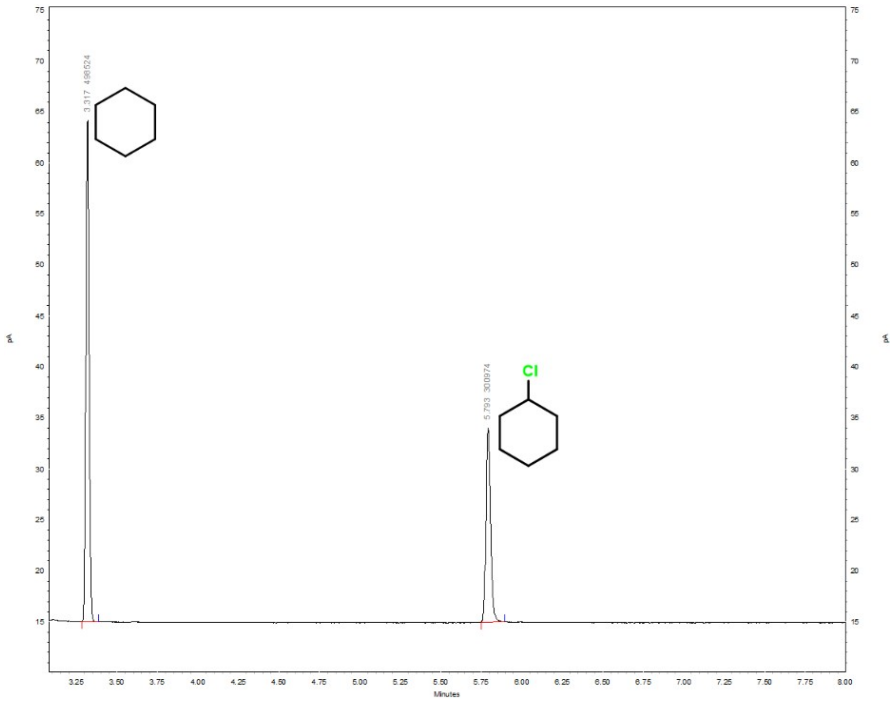

Fig. S20 GC trace for oxidation of cyclohexane using **1** in presence of 1 eq AcOH (X axis: in minute; Y axis: % abundance), entry 1 in Table 3.

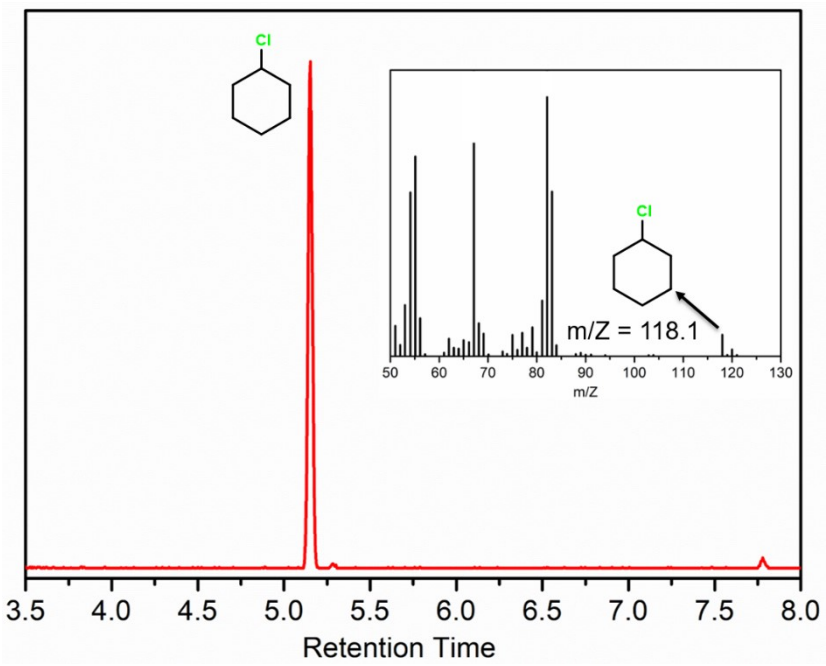

Fig. S21 GC-MS trace for oxidation of cyclohexane using **1** in presence of AcOH (X axis: in minute; Y axis: % abundance). Inset shows the GC-MS spectra for chlorocyclohexane.

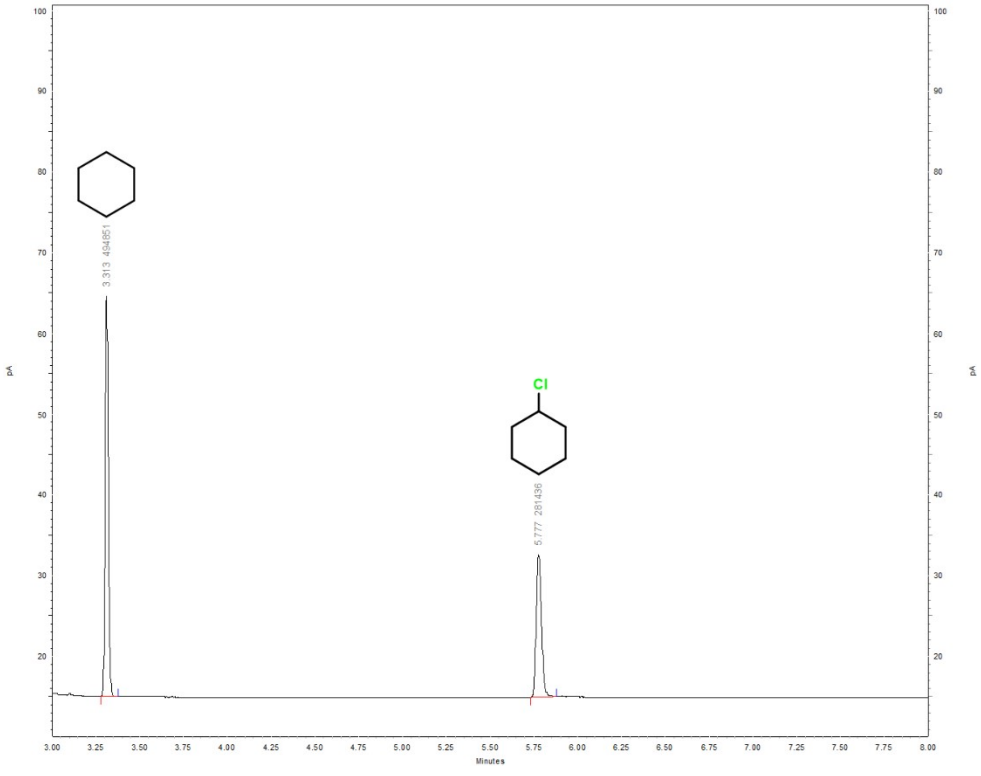

Fig. S22 GC trace for oxidation of cyclohexane using **2** in absence of AcOH (X axis: in minute; Y axis: % abundance).

Fig. S23 GC trace for oxidation of cyclohexane using **2** in presence of AcOH (X axis: in minute; Y axis: % abundance).

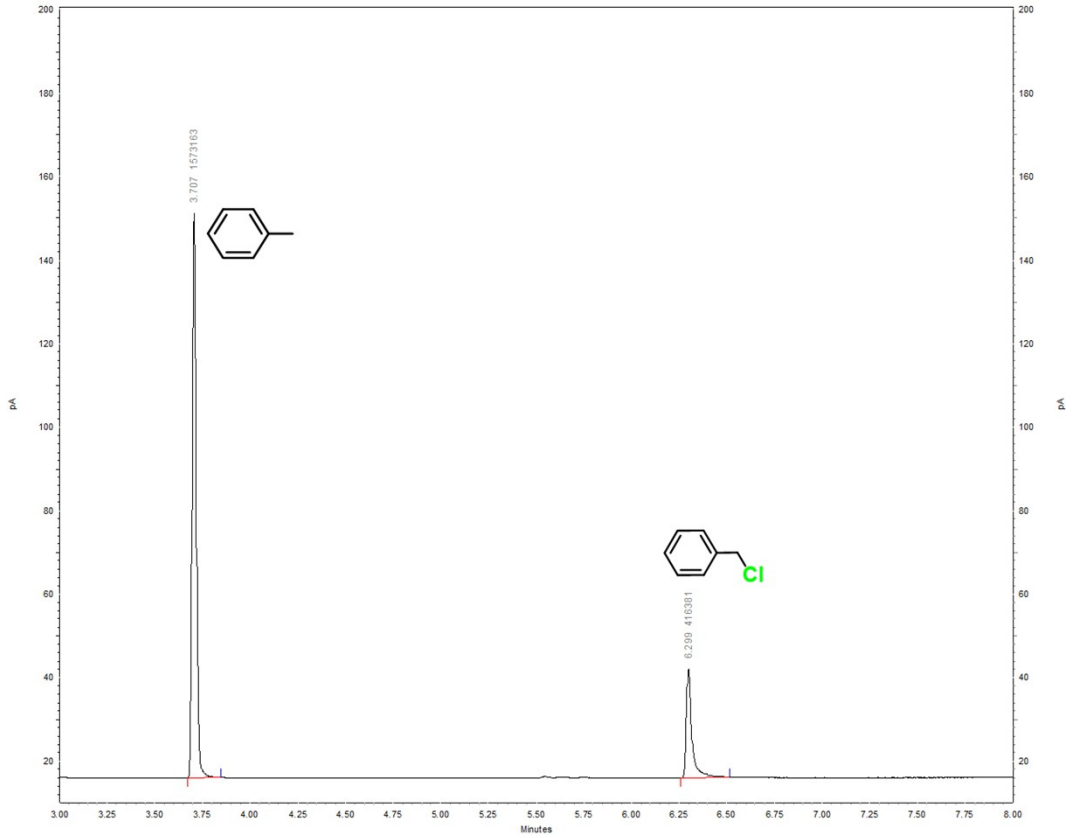

Fig. S24 GC trace for oxidation of toluene using **1** in presence of AcOH (X axis: in minute; Y axis: % abundance), entry 2 of Table 3.

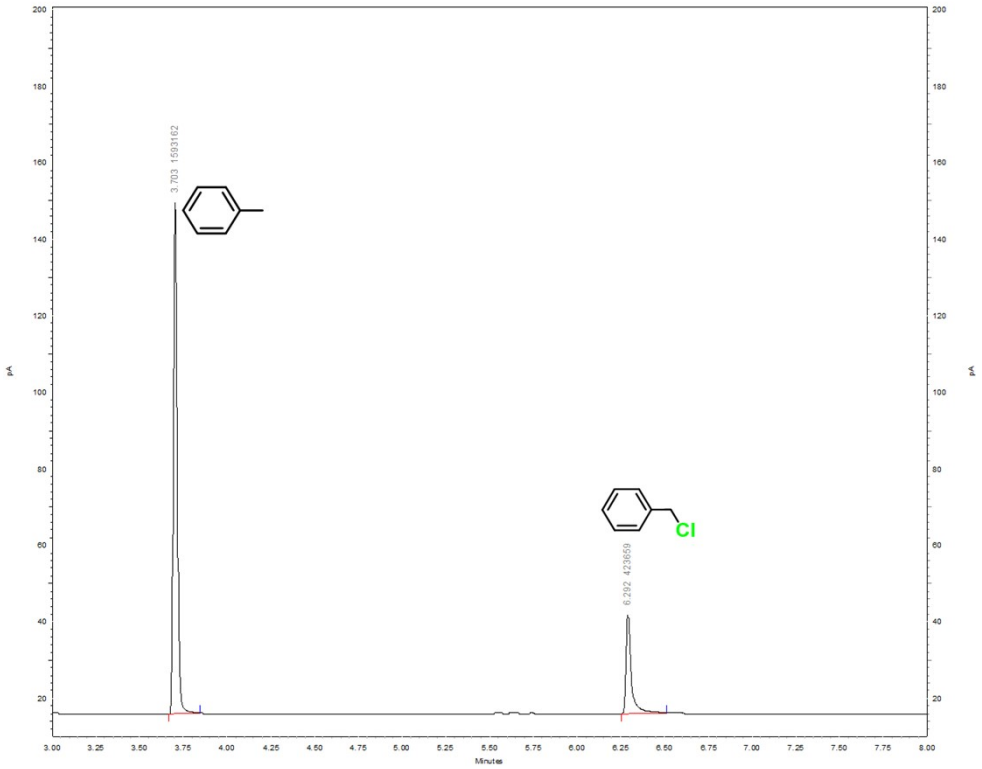

Fig. S25 GC trace for oxidation of toluene using **2** in absence of AcOH (X axis: in minute; Y axis: % abundance), entry 2 of Table 3.

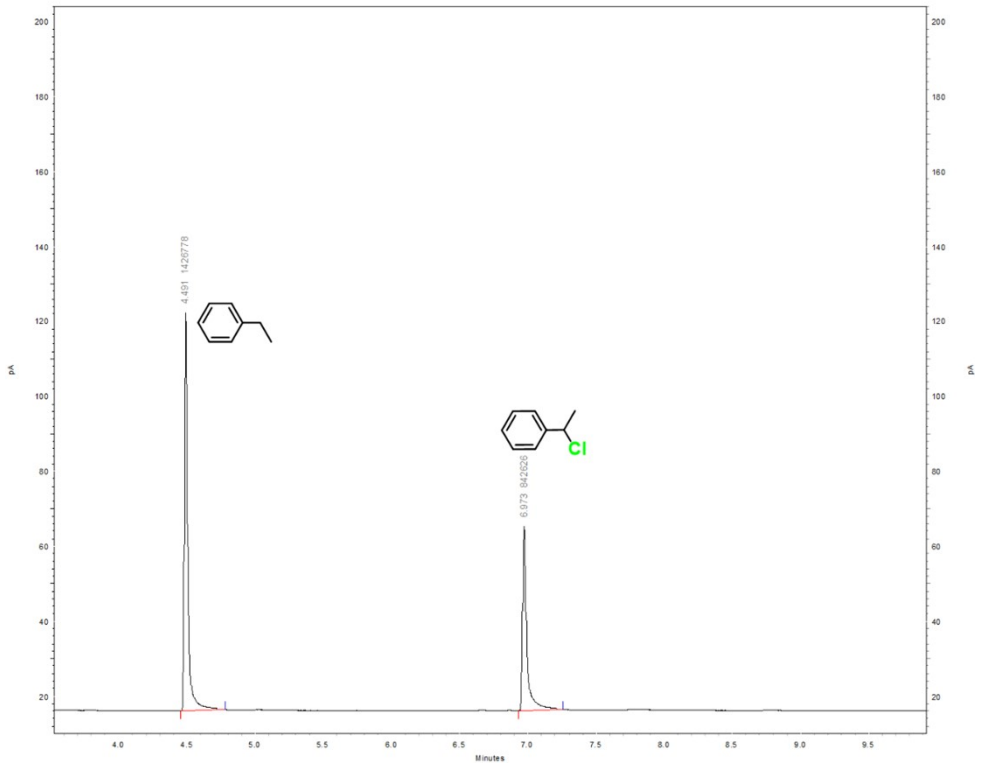

Fig. S26 GC trace for oxidation of ethyl benzene using **1** in presence of AcOH (X axis: in minute; Y axis: % abundance), entry 3 of Table 3.

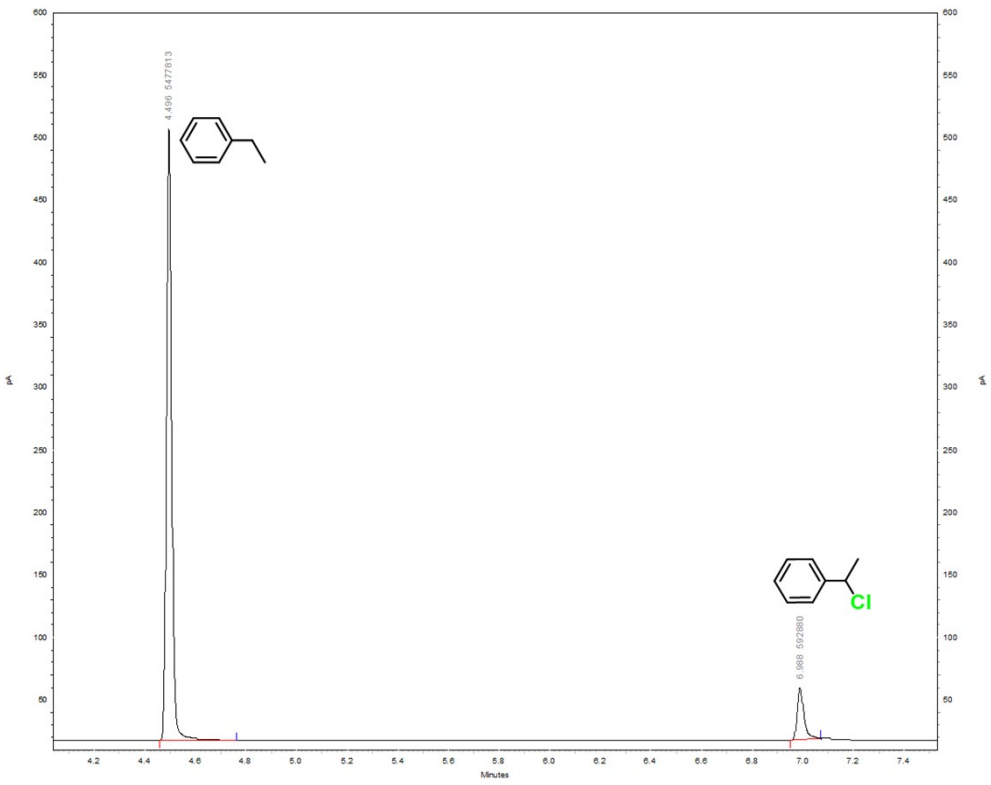

Fig. S27 GC trace for oxidation of ethyl benzene using **2** in presence of AcOH (X axis: in minute; Y axis: % abundance), entry 3 of Table 3.

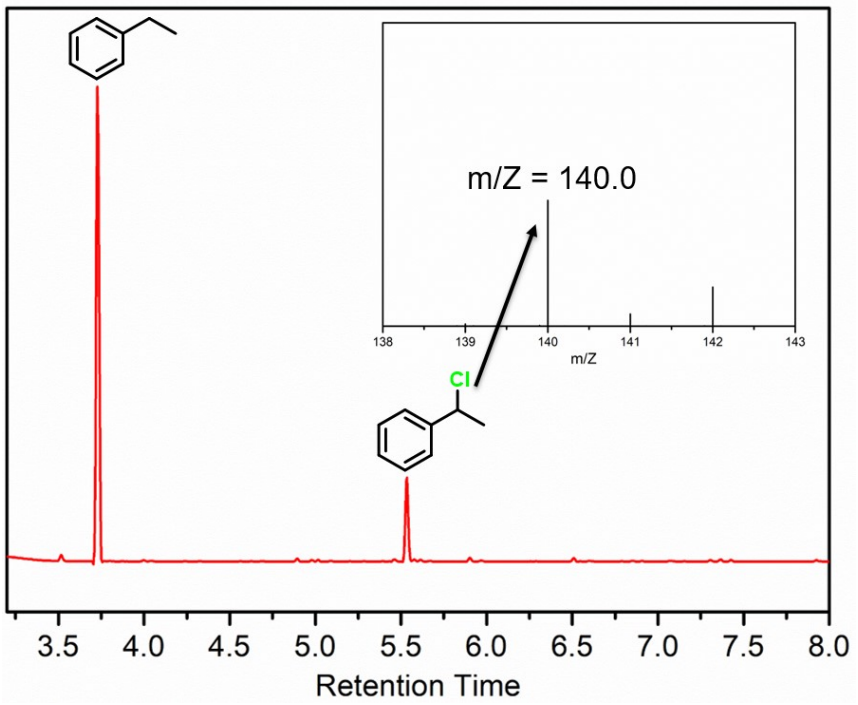

Fig. S28 GC-MS trace for oxidation of ethyl benzene using **1** in presence of AcOH. Inset shows the GC-MS spectra for (1-chloroethyl)benzene, entry 3 of Table 3.

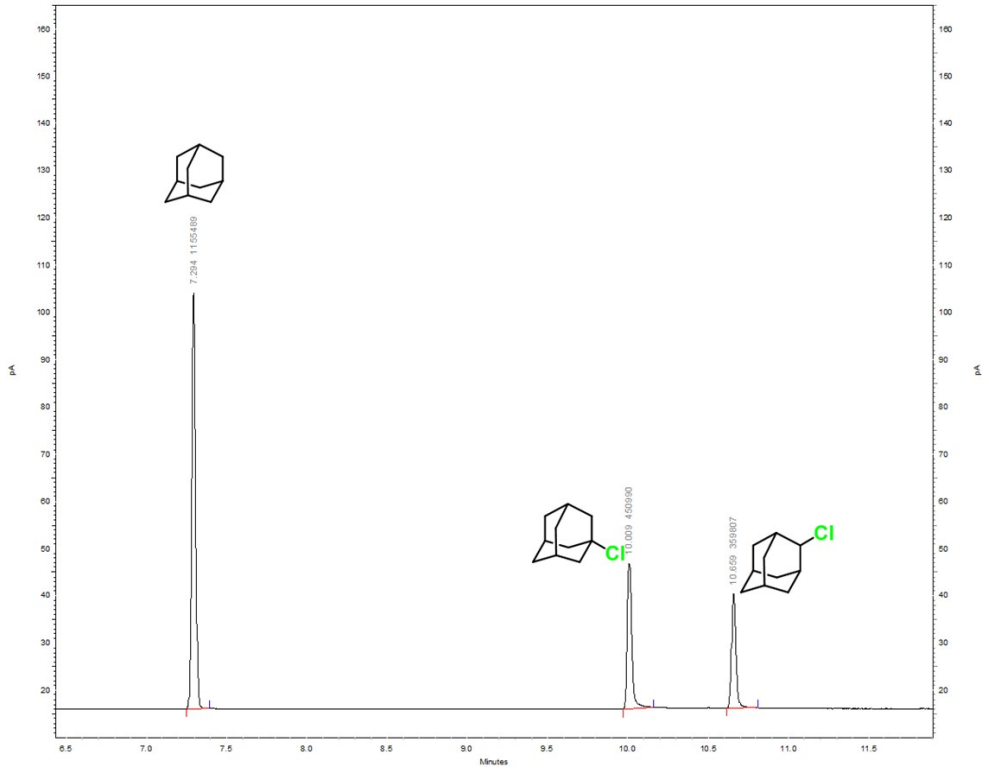

Fig. S29 GC trace for oxidation of adamantane using **1** in presence of AcOH (X axis: in minute; Y axis: % abundance), entry 4 of Table 3.

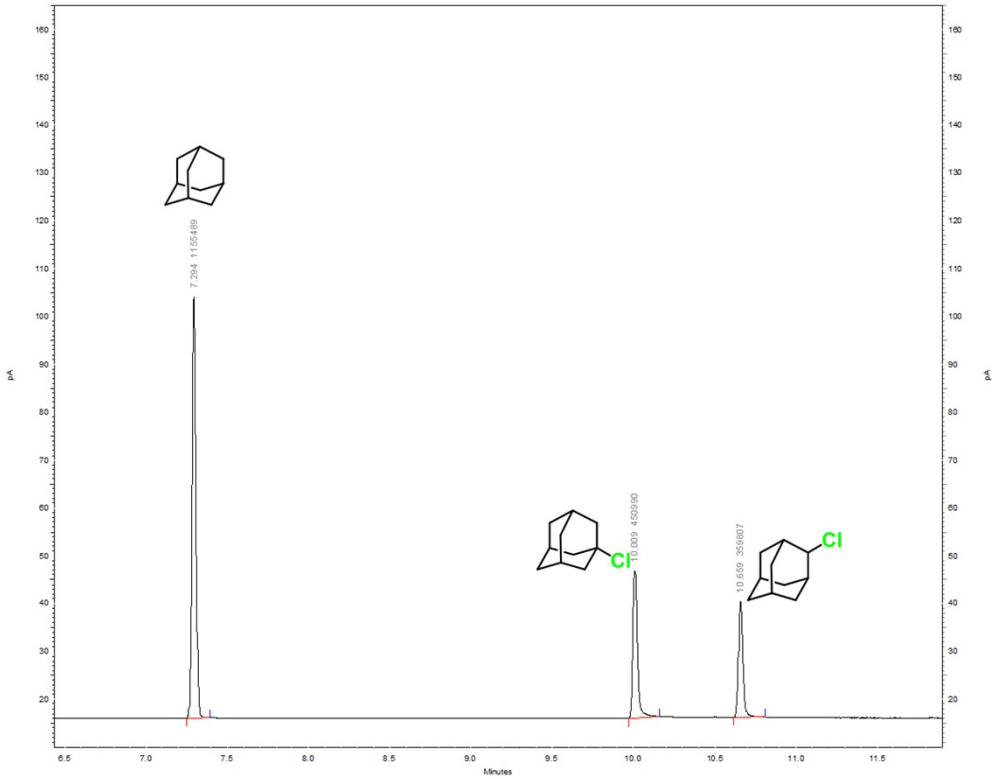

Fig. S30 GC trace for oxidation of adamantane using **2** in presence of AcOH (X axis: in minute; Y axis: % abundance), entry 4 of Table 3.

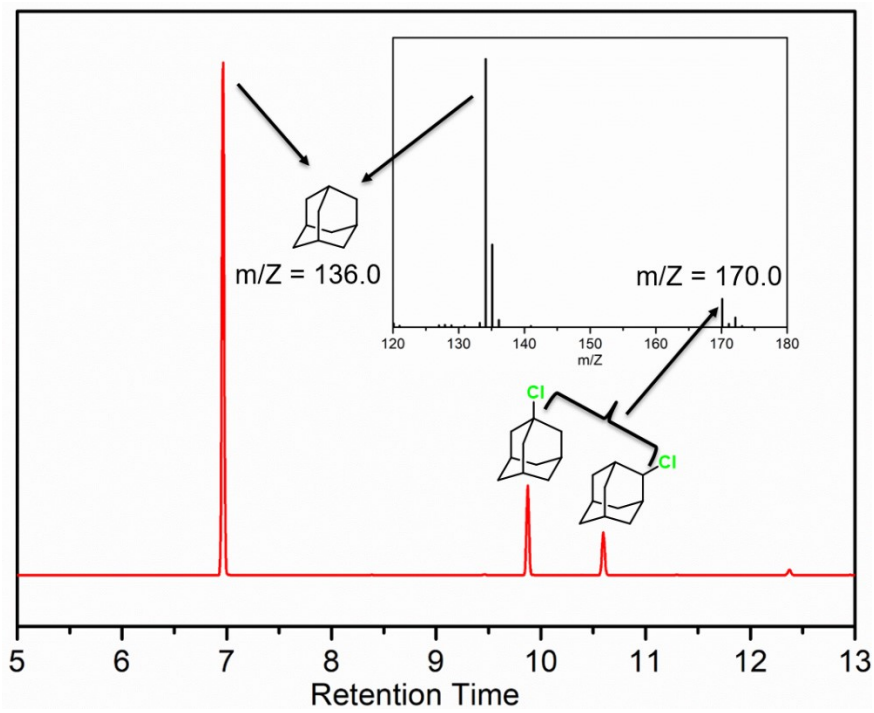

Fig. S31 GC-MS trace for oxidation of aadamantane using **1** in presence of AcOH. Inset shows the GC-MS spectra for1-chloroadamantane and 2-chloroadamantane.

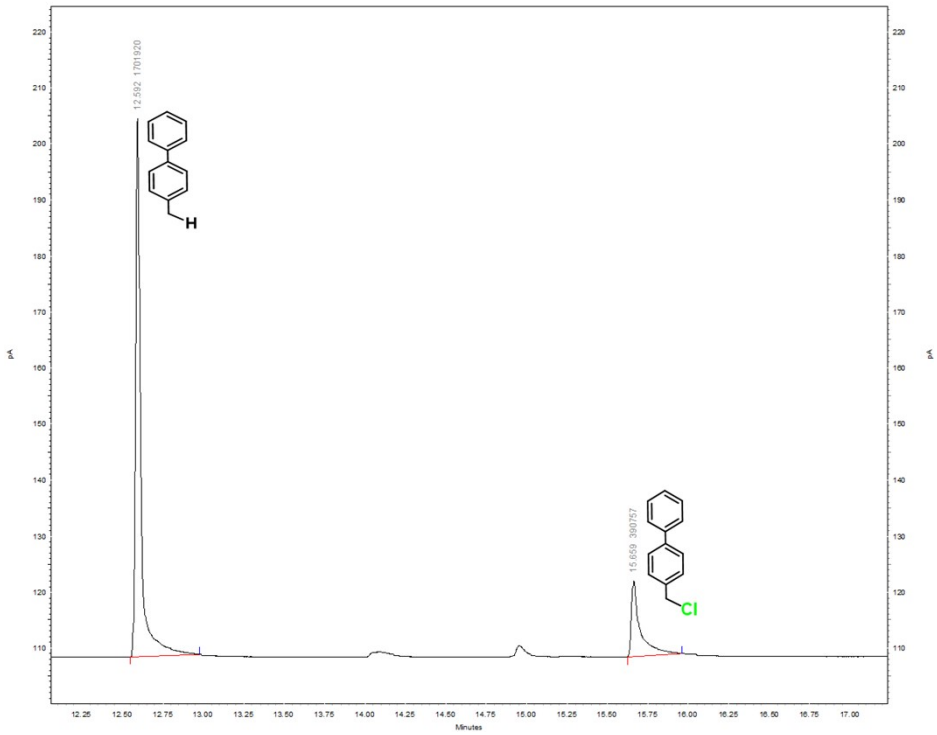

Fig. S32 GC trace for oxidation of 4-methyl biphenyl using **1** in presence of AcOH (X axis: in minute; Y axis: % abundance), entry 5 of Table 3.

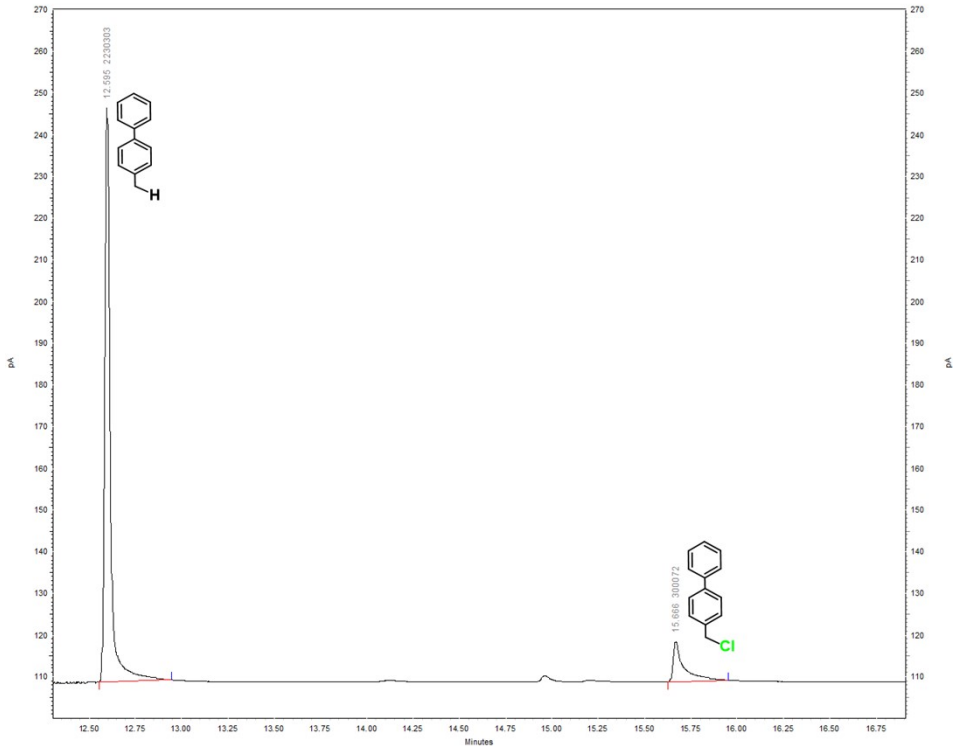

Fig. S33 GC trace for oxidation of 4-methyl biphenyl using **2** in presence of AcOH (X axis: in minute; Y axis: % abundance), entry 5 of Table 3. The peak at 15 minute was unidentified.

Spectroscopic characterization of the Ni(III) intermediates

Electron Paramagnetic Resonance (EPR) spectroscopy were recorded in conventional Bruker spectrometer (Bruker, EMXmicro) operating at X-band frequency and magnetic field modulation of 100 kHz, with a microwave power of 2.25 mW and modulation amplitude of 1 G at 100 K. The resonance lines were simulated by the Bruker WINEPR SimFonia program. The EPR spectra of the Ni(III) intermediates were recorded on a frozen solution of CH_3CN (1mM) in an EPR tube by adding 5 eq. NaOCl (20 µL, 50 mM) and 5eq. AcOH (20 µL, 50 mM). The respective EPR spectra are shown in Fig. 2B and S36. Other than EPR, Ni(III) intermediates were characterized by UV-Vis (Fig. S34) and HR-MS (Fig. S36).

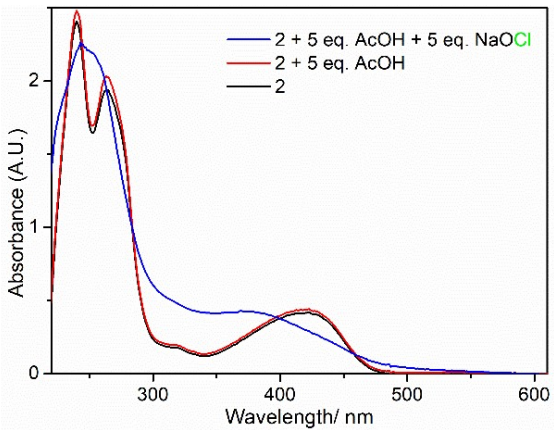

Fig. S34 UV-Vis spectral changes of complex (**2**) (0.1mM) on addition of 5 eq. AcOH and 5 eq. NaOCl.

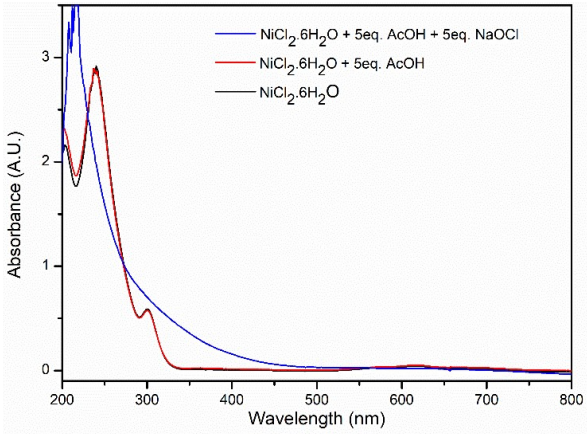

Fig. S35. UV-Vis spectral changes of $NiCl_2.6H_2O$ (1mM) on addition of 5 eq. AcOH and 5 eq. NaOCl.

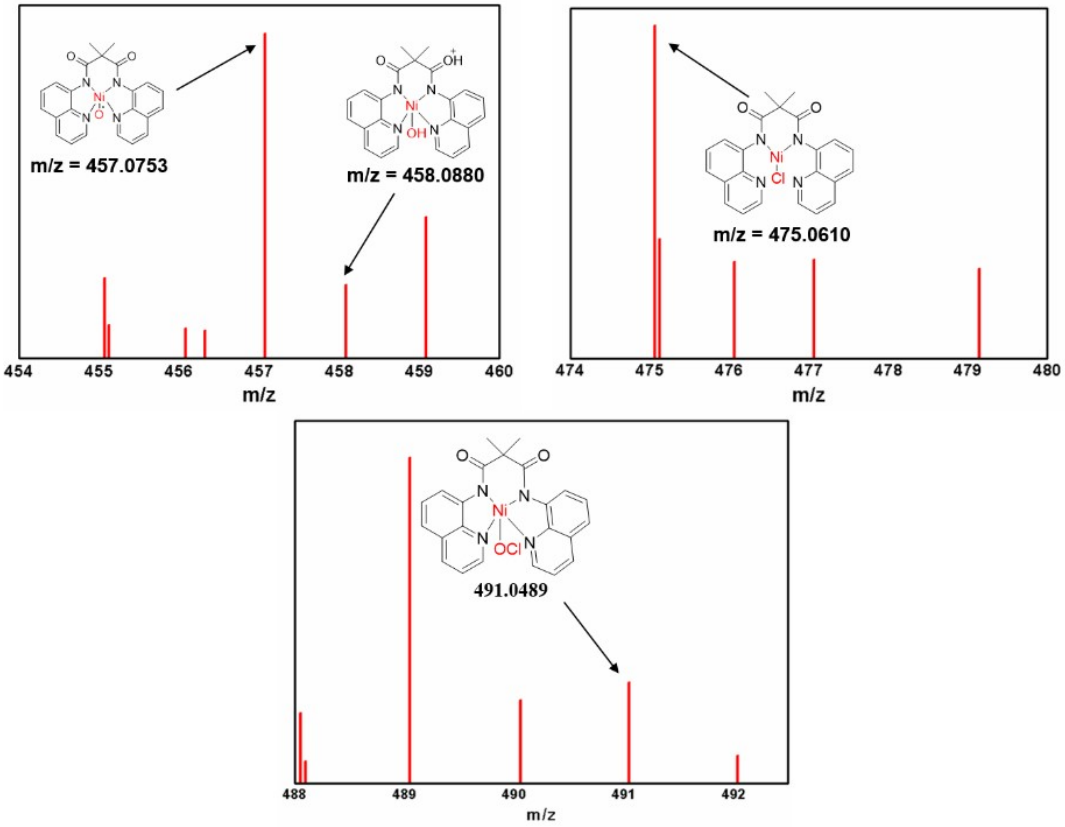

Fig. S36. HR-MS spectrum of high-valent Ni(III) intermediates on addition of 5 eq. AcOH and 5 eq. NaOCl.

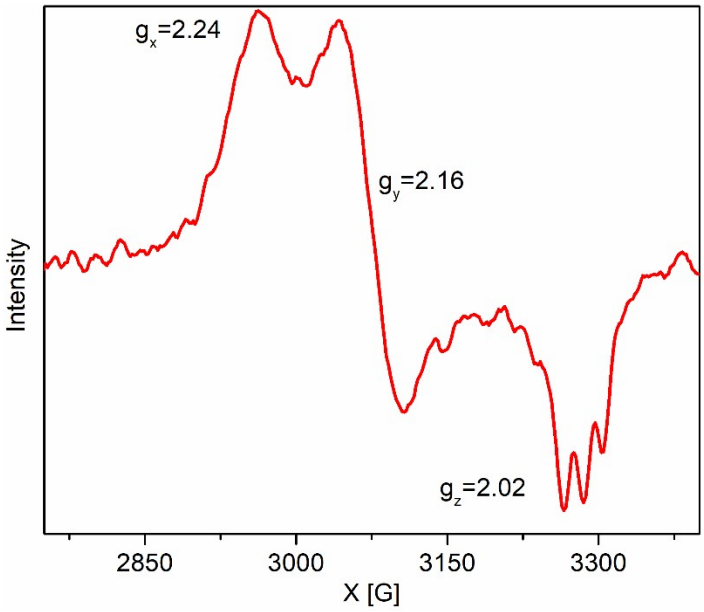

Fig. S37. EPR spectrum of complex (**2**) (1mM) on addition of 5 eq. AcOH and 5 eq. NaOCl.

Kinetic Analysis

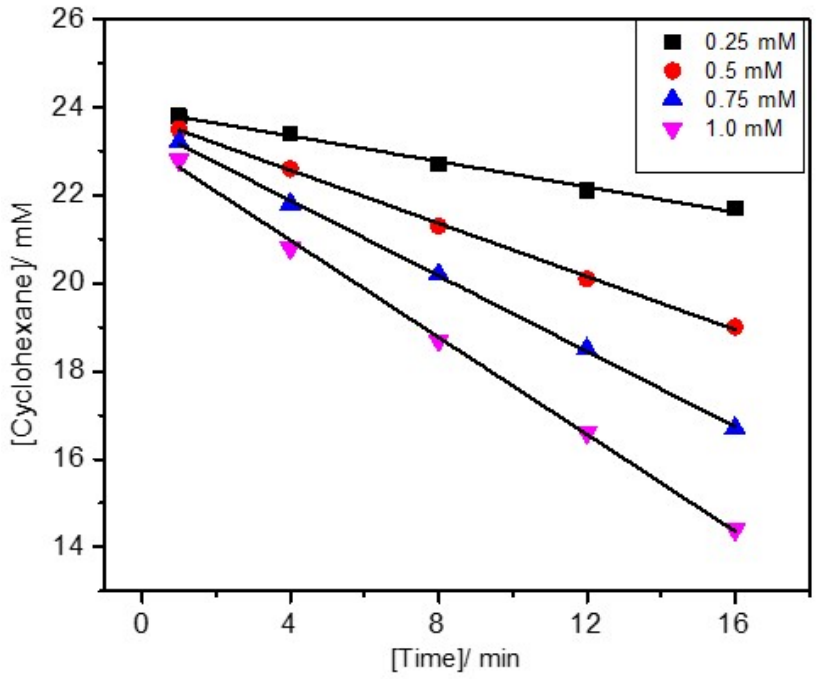

Fig. S38 Initial rate measurement for [**1**] variation (0.25 – 1 mM). [Cyclohexane] = 250 mM, [NaOCl] = 250 mM, Temperature ~25 ^{o}C, CH_3CN:CH_2Cl_2 (8:2 v/v) 1mL. During GC analysis, the reaction mixture was diluted 10 times. Each data point was the average of three reaction sets measured in GC.

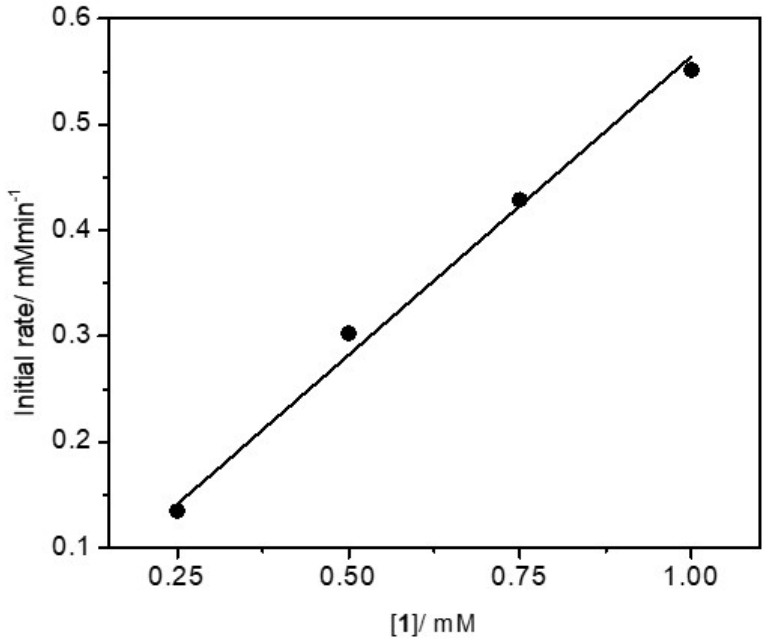

Fig. S39 Initial rate *vs*. [**1**].

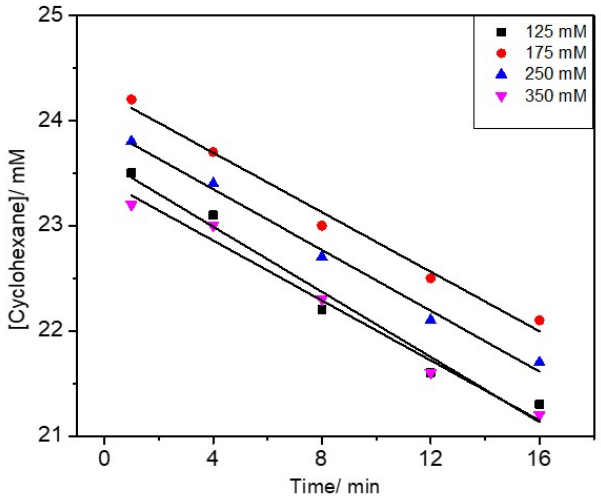

Fig. S40 Initial rate measurement for [NaOCl] variation (125 – 350 mM). [Cyclohexane] = 250 mM, [**1**] = 0.25 mM, Temperature ~25 ^{o}C, CH_3CN:CH_2Cl_2 (8:2 v/v) 1mL. During GC analysis, the reaction mixture was diluted 10 times. Each data point was the average of three reaction sets measured in GC.

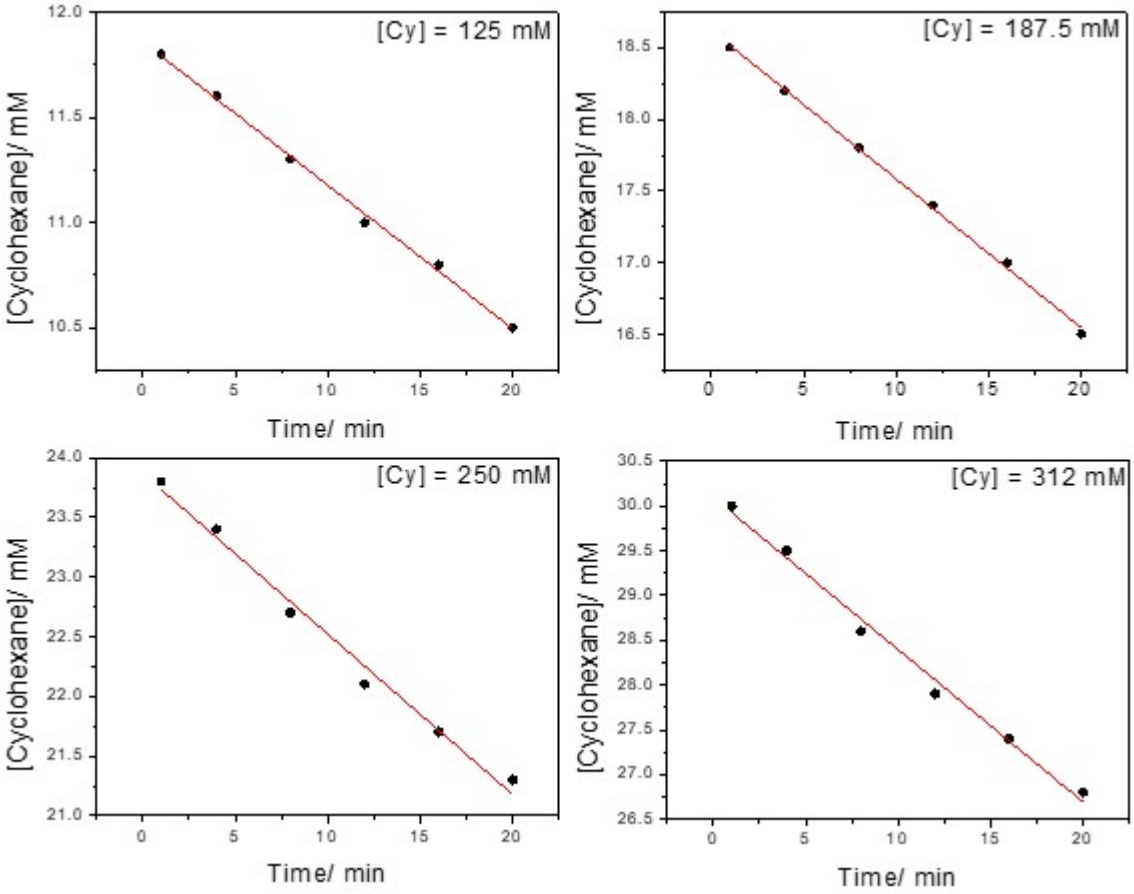

Fig. S41 Initial rate measurement for [cyclohexane] variation (125 – 312 mM). [1] = 0.25 mM, [NaOCl] = 250 mM, Temperature ~25 °C, CH_3CN:CH_2Cl_2 (8:2 v/v) 1mL. During GC analysis, the reaction mixture was diluted 10 times. Each data point was the average of three reaction sets measured in GC.

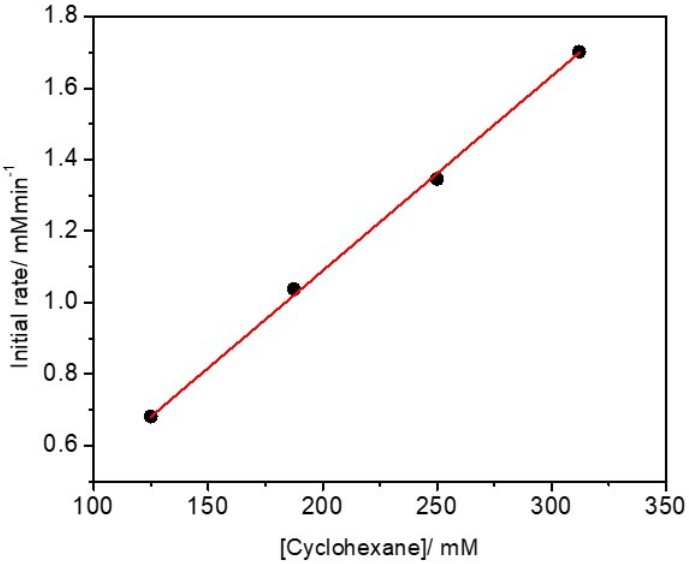

Fig. S42 Initial rate *vs*. [Cyclohexane].

Table S4 TOF of **1** in catalytic chlorination of alkanes with NaOCl. Conditions: [NaOCl] = 250 mM, [1] = 0.25 mM, for cyclohexane, toluene and ethylbenzene concentration was kept at 250 mM while for 2,3-dimethyl butane it was 300 mM, Temperature ~25 °C, CH_3CN:CH_2Cl_2 (8:2 v/v) 1mL.

entry	substrate	BDE (kcal mol^{-1})	V_i × (mM min^{-1})	TOF (min^{-1})	k_2 (M^{-1} min^{-1})	k_2' (M^{-1} min^{-1})
1	cyclohexane	99.3/5	1.37	5.50	2.20×10^{-5}	1.83×10^{-6}
2	toluene	90.0/89.7	1.49	5.96	2.38×10^{-5}	7.93×10^{-6}
3	ethyl benzene	87.0	1.35	5.40	2.16×10^{-5}	1.08×10^{-5}
4	2,3-dimethyl butane	96.5	0.66	2.67	8.90×10^{-6}	4.45×10^{-6}

Table S5 Comparison of Catalytic Activity of Various Catalysts for C-H chlorination of cyclohexane with NaOCl.

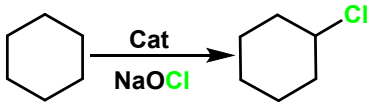

Entry	Catalyst	Time (h)	Temp (°C)	$TON_{chlorination}$	Ref. in the manuscript
1	**Ni^{II}(L)**	0.5	RT	212	This work
2	[Ni^{II}(L)] (L = bis-amidate ligand)	2	-30	44	11
3	[Ni^{II}(Pytacn)$(CF_3SO_3)_2$ [(Pytacn = 1-(2-pyridylmethyl)-4,7-dimethyl-1,4,7-triazacyclononane)	2	RT	24	10
4	Mn(TPP)Cl/NaOCl	2	RT	87	7

Determination of the Kinetic Deuterium Isotope Effect (KIE)

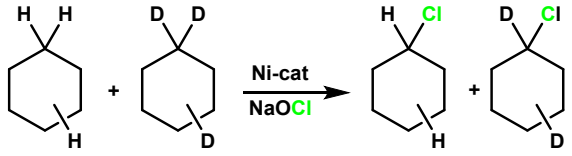

A mixture of cyclohexane (50 µmol) and cyclohexane-d_{12} (50 µmol) were added to a solution of the Ni-catalyst (**1** and **2**) (0.25 µmol) in CH_2Cl_2/CH_3CN (2:8 v/v) 1mL under N_2. Then, acetic acid (50 µmol) and NaOCl (50 µmol) were added slowly using gas tight syringe to the reaction mixture and it was stirred at RT for 30 minutes. Finally, the reaction mixture was passed through a solution through a short plug of neutral alumina. The product distribution was calculated by GC-MS. The kinetic isotope effect (KIE) value for chlorocyclohexane production was calculated by (moles of chlorocyclohexane)/(moles of chlorocyclohexane-d_{11}) (Ratio = 2 = $K_{H/D}$).

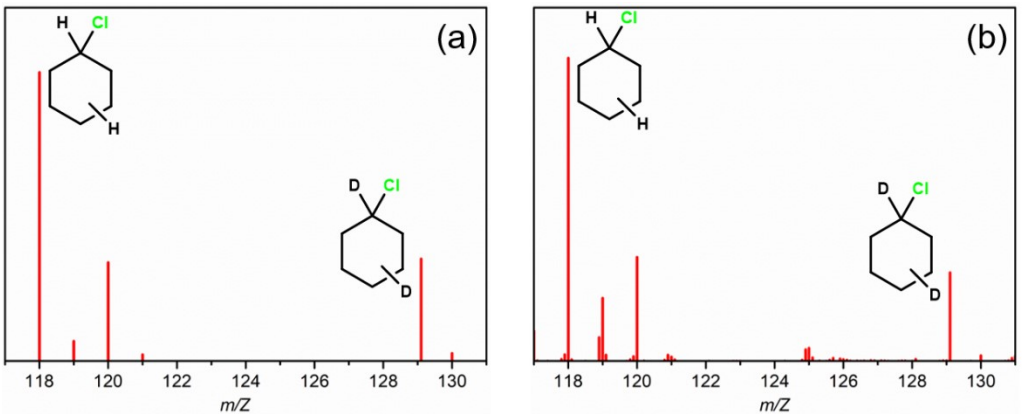

Fig. S43 Isotope patterns of chlorocyclohexane and d_{11}-chlorocyclohexane on the GC-MS spectra obtained after 30 minutes in the reaction of cyclohexane (50 μmol) and cyclohexane-d_{12} (50 μmol) with NaOCl (50 μmol), acetic acid (50 μmol) catalyzed by **1** (0.25 μmol) (a) and **2** (0.25 μmol) (b) under the reaction conditions described in the text.

References

1. Bruker Support APEX3, SAINT, and SADABS: Software for data reduction, absorption correction and structure solution; Bruker AXS Inc.: Madison, WI, USA, 2015; http://www.brukersupport.com/
2. G. M Sheldrick, SHELXTL Version 2014/7: Programs for the Determination of Small and Macromolecular Crystal Structures by Single Crystal X-ray and Neutron Diffraction; University of Göttingen, Göttingen, Germany, 2014; http://shelx.uni-ac.gwdg.de/SHELX/index.php.
3. G. M Sheldrick. A short history of SHELX. *Acta Crystallogr*., Sect. A: Found. Crystallogr. 2008, **64**, 112−122.
4. L. J. Farrugia, ORTEP-3 for Windows - a version of ORTEP-III with a Graphical User Interface (GUI). *J. Appl. Crystallogr*. 1997, **30**, 565.